Energy Syst (2019) 10:821–842
https://doi.org/10.1007/s12667-018-0293-9

ORIGINAL PAPER

An improved adaptive wide-area load shedding scheme for voltage and frequency stability of power systems

Kazem Mehrabi[1] · **Sajjad Golshannavaz**[2] · **Saeed Afsharnia**[1]

Received: 14 October 2017 / Accepted: 18 May 2018 / Published online: 22 May 2018

Abstract Conventional under-frequency and under-voltage load shedding schemes are known as effective approaches for load shedding purposes. Generally, these two schemes are deployed independently within which the combinatorial disturbances are overlooked. Contributing to this context, the ongoing study raises a high concern on developing a generalized wide-area adaptive load shedding scheme. In order to preserve the voltage and frequency stabilities, the established approach deploys the variations of voltage, frequency, active, and reactive power in all buses, simultaneously. More specifically, the reactive power variation on voltage stability is incorporated in the proposed load shedding index. This idea improves the performance of the proposed scheme, significantly. Infield phasor measurement units are establishing a wide-area basis, enabling the proposed approach in modern control centers. Extensive numerical studies are devised to assess the performance of the proposed approach encountering various disturbances. The obtained results are discussed in depth.

Keywords Adaptive load shedding scheme · Under-frequency load shedding (UFLS) · Under-voltage load shedding (UVLS) · Wide area measurement system (WAMS) · Phasor measurement unit (PMU)

✉ Sajjad Golshannavaz
s.golshannavaz@urmia.ac.ir

Kazem Mehrabi
mehrabi.kazem@ut.ac.ir

Saeed Afsharnia
safshar@ut.ac.ir

1 School of ECE, University of Tehran, Tehran, Iran

2 Electrical Engineering Department, Urmia University, Urmia, Iran

List of symbols

L	Total overload
LD	Total amount of load to be shed
d	Load reduction factor
$f,\ df/dt$	Frequency and its rate of change
f_{min}	Minimum permissible frequency
f_n	Power system nominal frequency
f_c	Frequency of the equivalent inertial centre
$f_{setting}$	Frequency setting in load shedding scheme
N	Total number of generators
H_i	Inertia constant in ith generator (s)
ε	Constant value
m	The boundary amount for differentiating the small and large disturbances
ΔP	Generation-consumption mismatch
P, Q	Active and reactive powers
V	Bus voltage magnitude
i, k	Bus indices
θ	Bus voltage angle
E	Thevenin equivalent network voltage
Z_{Thev}	Thevenin equivalent network impedance
Q_{Thev}	Thevenin equivalent generator reactive power
VSI	Voltage stability index
QSI	Reactive power stability index
$QVSI$	Reactive power-voltage stability index
Q_L	Total reactive power consumption at each bus
P_m	Generator's mechanical power
P_e	Generator's electrical power
P_{shed}	Amount of load to be shed
P_{thr}	Power as spinning reserve
DF_1, DF_2	Lower and upper bounds of frequency variations
J	Jacobian matrix
J_R	Reduced Jacobian matrix
E_L	Left eigenvector of J_R
E_R	Right eigenvector of J_R
ξ	Diagonal eigenvalue of J_R
$E_{L,l}$	l-th row of E_R
$E_{R,l}$	l-th column of E_R
λ_l	l-th eigenvalue of J_R
ΔV_{ml}	Variation of l-th modal voltage
ΔQ_{ml}	Variation of l-th modal reactive power
VQS_k	V–Q sensitivity at bus k
$\mu_{k,l}$	k-th element of $E_{R,l}$
$\eta_{l,k}$	k-th element of $E_{L,l}$

1 Introduction

The economical/environmental restrictions are regarded as the main obstacles in expanding new electric grids for accommodating the increased demanded power. Thus, the existing networks and infield components are operated close to their maximum capacities. This, in turn, depreciates the desired stability margins. In such conditions, the generators or tie-lines outages instigate the generation-consumption mismatches and thus, the power system stability jeopardizes [1–5].

The load shedding is well-regarded as a last resort in maintaining the power system stability which is divided to two protective methods based on frequency and voltage collapses [6]. This mechanism is mainly triggered in the systems where the spinning reserve quantities are not sufficient to preserve the balance of production and consumption [7]. Under-frequency or under-voltage relays are well-recognized as initial elements in load shedding process. Under-frequency load shedding (UFLS) is mainly dealing with the frequency stability of the power system, above the permissible minimum threshold. The initial implementation of this approach was established in North-eastern blackout, occurred in 1965. In technical representations, the conventional UFLS strategy deploys the gradual shedding of loads to avoid the power system instability [8–10]. Minimizing the amount of load shedding process by islanding the network is an idea proposed by the authors in [11, 12]. Authors in [13] have been proposed a controlled load shedding process to prevent the overall blackouts. In a similar manner, the UVLS technique is effective in avoiding the power system voltage collapse [14, 15]. These approaches, although demonstrating acceptable functionalities, are exposed to some technical defects, some of which could be named as follows:

The frequency settings of relays are adjusted at predetermined and constant values. As well, the amount of shed load at each step is constant and not adapted for different disturbances. The intentional time-delay setting which prevents the relay from responding to transient signals are similar for both the small and large disturbances. The combinational frequency and voltage instabilities are overlooked within which the conventional load shedding strategies lose their validities. In the case of large disturbances, the load shedding steps might be disturbed with each other. In these methods, the concurrent voltage and reactive power variations at all buses are not considered and thus, the instability is mainly contributed to the gradual load increase.

To avert such issues, a high attention has been paid for improving the conventional load shedding schemes. In this way, adaptive load shedding strategies are proposed, sensibly. These approaches are mainly characterized with higher flexibility and capability in allocating proper settings, control actions, and shed loads encountering different disturbances. These methods are categorized in twofold: response-based and event-based approaches. Although some effective attempts are made, however, a few efforts are dealing with fine tuning of relays. In this context, some studies have concentrated on intentional reducing of time-delay setting, adopted for larger disturbances accompanied with greater df/dt. As well, some other researchers have proposed the application of frequency signal and its rate of change, indicated by f and df/dt [16–19]. Considering the possible instabilities, references [20, 21] have considered the voltage variations to determine proper load shedding decisions. Instead of using the power swing equations to determine the active power mismatches, in

[22] an off-line stochastic analysis has been proposed. However, the off-line analyses and neglecting the voltage stability indices could steer the system toward unstable situation. In [23], the ratio of active power variations to voltage deviations is used as an index for load shedding task. However, it is well-recognized that the voltage displacements are substantially depended to reactive power variations. Furthermore, authors in [24] have suggested a new load shedding scheme based on artificial neural networks. The main flaw regarding the intelligent and heuristic approaches is their partial extensibility to accommodate the changes in operating points. Thus, a reliable load shedding manner is not granted. As well, in order to enhance the voltage stability of the power system, in [25–28] the voltage stability index (VSI) has been considered instead of voltage magnitude index. The most challenging point herein is the extraction of the Thevenin equivalent generator voltage and impedance. Hence, the practical implementation of such remedies is difficult. What is more, the investigated literatures do not incorporate all the opportunities provided by the wide-area infrastructure of modern power systems. Further in this context, the Modal analysis is recognized as an effective method founded for adaptive load shedding practice. This method utilizes the Jacobian matrix to select the most potent buses prone to instability occurrence [29, 30]. The main drawback for this strategy is its high computational burden and time-consuming nature which degrades it as a suitable online method.

Based on the preceding survey, this manuscript proposes an adaptive wide-area load shedding scheme to enhance both the voltage and frequency stabilities. The proposed approach gets access to the overall wide-area system data from PMUs. The important signals at each bus namely, the voltage magnitude, frequency and its rate of change, active and reactive powers are accommodated to form the proposed shedding index. Thus, following the adaptive tuning of frequency thresholds, the most potent buses which are prone to instability are determined. Then, these buses are included in the load shedding process to preserve the system stability. To make it brief, the followings could be mentioned as the main contributions of the proposed approach:

In contrast to the available mechanisms, the frequency thresholds of load shedding relays are adaptively adjusted. This task is performed in a wide-area manner. Hence, an improved load shedding strategy is observed for frequency stability enhancement. Fast changes in both the reactive power and voltage magnitude in all buses are effectively considered. This issue is more significant for particular loads within which the voltage instability is more likely. The wide-area low computational burden of the proposed approach results in a fast-response shedding operation. Thus, an effective approach is achieved for stability enhancement.

The remainder of this paper is organized as follows. Section 2 reviews the conventional and adaptive load shedding schemes and provides a technical comparison basis. Section 3 addresses the proposed approach in details and founds the contemplated mathematical framework. The investigated test system and several numerical analyses are interrogated in Sect. 4. Eventually; the general discussions and concluding remarks are portrayed in Sect. 5.

2 The adaptive versus conventional load shedding schemes

2.1 Conventional schemes

In these schemes, if the system frequency drops down the predetermined permissible range, the load shedding task is initiated. Following each disturbance, the per-unit overload value is calculated based on Eq. (1). Then, at each step, the amount of shed load is determined based on Eq. (2).

$$L = \frac{Total\ Load - Total\ Generation}{Total\ Generation} \tag{1}$$

$$LD = \frac{\frac{L}{L+1} - d\left(1 - \left(\frac{f_{\min}}{f_n}\right)\right)}{1 - d\left(1 - \left(\frac{f_{\min}}{f_n}\right)\right)} \tag{2}$$

Here, parameter d models the load's dependency to frequency variations. Afterwards, the computed shed load, denoted by LD, is applied in several constant steps [31].

The predetermined and constant settings of relays and shed load at each step, the constant intentional time-delay setting for both the small and large disturbances and the neglecting of combinational frequency and voltage instabilities are issues that to avert such problems, a high attention is paid for improving the conventional load shedding schemes. In this way, adaptive load shedding strategies are proposed, sensibly.

2.2 Adaptive load shedding schemes

2.2.1 Response-based approach

This approach incorporates the network's status along with the generators' swing equations to reach in a fine approximation of generation-consumption mismatches. Equations (3)–(8) are the mathematical statements of this approach. The swing equation in each generator is modeled by Eq. (3).

$$\frac{2H_i}{f_n}\frac{df_i}{dt} = P_{m_i} - P_{e_i} = \Delta P_i \ (i = 1, \ldots, N) \tag{3}$$

This equation is extended to consider the total generation-consumption mismatches in all generators, represented by Eq. (4).

$$\Delta P = \sum_{i=1}^{N} \Delta P_i = \frac{2\sum_{i=1}^{N} H_i}{f_n}\frac{df_c}{dt} = \varepsilon\frac{df_c}{dt} \tag{4}$$

The equivalent inertial centre frequency, indicated by f_c, and also the parameter ε are calculated based on Eqs. (5) and (6), respectively.

$$f_c = \frac{\sum_{i=1}^{N} H_i f_i}{\sum_{i=1}^{N} H_i} \tag{5}$$

$$\varepsilon = \frac{2}{f_n} \sum_{i=1}^{N} H_i \tag{6}$$

Subsequently, some of the recorded mismatches are afforded with the generation reserve capacities. However, the remaining amount experiences a forced load shedding process, represented by Eq. (7).

$$P_{shed} = 1.05 \times (\Delta P - P_{thr}) \tag{7}$$

The tripped generator might also have been scheduled to provide a specific amount of reserve capacity. However, its outage decreases the available reserve power. To bridge this technical gap and to enhance the reliability issues, the factor of 1.05 is included in this equation. In some cases, this amendment results in negligible increase of shed load, as compared to the conventional methods. In this approach, two threshold frequencies are considered to adaptively adjust the frequency settings in small and large disturbances. This view is represented by Eq. (8). The large disturbances with higher df/dt are properly managed by 49.7 Hz, as the frequency threshold. This is while; a lower value is settled on 49.4 Hz for small disturbances.

$$f_{setting} = \begin{cases} 49.7 \ \ \frac{df}{dt} \geq m; \text{ large disturbance} \\ 49.4 \ \frac{df}{dt} < m; \text{ small disturbance} \end{cases} \tag{8}$$

In the preceding equation, m represents the boundary rate of frequency derivative in small and large disturbances. Any particular system could preserve its stability up to a specified generation outage. The recorded df/dt is, then, determined as the boundary value of m for differentiating the small and large disturbances. Although the load shedding process is triggered based on the system frequency and its changing trend, however, the buses with smaller voltage magnitudes are also concerned by the proposed approach. The adaptive mechanisms are shown to yield in a better stability response rather than the conventional schemes, particularly for large disturbances. However, the main flaw comes back to the selection approach of the buses with lower voltage magnitude. An improper selection task ends in power system instability, more evident in large and fast-propagated disturbances [32].

2.2.2 Load shedding based on modal analysis

In brief, the Modal analysis is addressed as follows. The linearized power flow is represented by Eq. (9). As there is no any strong correlation between the active

power and voltage magnitude variations, this dependency could be neglected. Thus, Eqs. (10)–(11) are achieved.

$$\begin{bmatrix} \Delta P \\ \Delta Q \end{bmatrix} = \begin{bmatrix} J_{P\theta} & J_{PV} \\ J_{Q\theta} & J_{QV} \end{bmatrix} \begin{bmatrix} \Delta\theta \\ \Delta V \end{bmatrix} \tag{9}$$

$$\Delta Q = \left[J_{QV} - J_{Q\theta} J_{P\theta}^{-1} J_{PV} \right] \Delta V = J_R \Delta V \tag{10}$$

$$\Delta V = J_R^{-1} \Delta Q \tag{11}$$

A mathematical decomposition of J_R^{-1} makes it possible to introduce the right and left eigenvectors, stated in Eq. (12). As well, by including the eigenvalues of J_R, this statement is renewed by Eq. (13).

$$J_R^{-1} = E_R \xi^{-1} E_L \tag{12}$$

$$\Delta V = E_R \xi^{-1} E_L \Delta Q = \sum_l \frac{E_{R,l} E_{L,l}}{\lambda_l} \Delta Q \tag{13}$$

Consequently, the l-th term in voltage variation Modal is obtained as follows:

$$\Delta V_{ml} = \frac{\Delta Q_{ml}}{\lambda_l} \tag{14}$$

Here, $\lambda_l \leq 0$ corresponds to the voltage instability recorded for a specific Modal. Making use of k-th element in right and left eigenvectors, the voltage sensitivity due to reactive power variations (VQS_k) is stated by Eq. (15).

$$VQS_k = \frac{dV_k}{dQ_k} = \sum_l \frac{\mu_{k,l} \cdot \eta_{l,k}}{\lambda_l} \tag{15}$$

How much the VQS_k value tends toward zero, that bus is more potent to instability occurrence [33, 34]. Although the Modal analysis is a renowned and well-defined scheme, however, it encounters some technical flaws. Some of the most serious concerns are stated as follows:

The requirement of eigenvalue vectors, Jacobin matrix, and also participation coefficients causes the Modal analysis to be featured with a high computational burden. To remove this barrier, the pre-fault network status is deployed to determine the load shedding regime. This point could be an origin of system instabilities, more evidently in large disturbances. This approach introduces the gradual load increase as the instability origin. Accordingly, some crucial issues such as the large and rapid loading variations are overlooked.

3 The proposed adaptive load shedding scheme

In references [25–28], the voltage magnitude is effectively deployed as an indicator of voltage instability. As well, authors in [33, 34] have proposed the concurrent

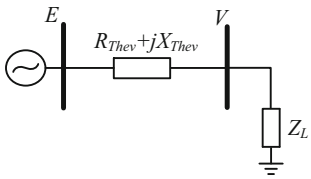

Fig. 1 The Thevenin equivalent network behind each bus

application of reactive power and voltage magnitude for determination of the most potent buses, prone to instability. These literatures have demonstrated the promising performance of voltage magnitude and reactive power variations in tracking the system stability issues. Thus, the authors are encouraged on making benefit of these two parameters in devising a new and effective index for stability investigations. Contemplating the general aspects of the investigated VSI in [35], an improved load shedding mechanism is proposed for retrieving the power system stability. The proposed approach is easily implemented considering the recently evolved wide-area measurement systems (WAMS). It is a well-recognized fact that the reactive power variation propagates more swiftly than the variations in voltage magnitude. Hence, as a new insight, the reactive power variations are wisely incorporated in determination of the most potent buses, prone to instability. Illustratively, Fig. 1 represents a typical two-bus power system behind a specific bus. The main idea is analogous to VSI scheme. Following any specific outage in generation units, the reserve capacity may not meet the generation-consumption balance, and thus, there may be a lack of reactive power. Accordingly, the buses which are close to the tripped generators are far from the remaining units and thus, adequate reactive power is not easily transferred, there. Considering several buses in close vicinity of each other, the buses which are faced with higher requirement of reactive power are more stressing the power system and thus, are identified as the most potent buses in regard of instability. Accordingly, in the established method, how much a greater reactive power is seen across the Thevenin equivalent impedance, that bus is more potent to stimulate the instability. Expectedly, a large voltage drop is also perceived among the equivalent impedance.

Given that the PMU data can be real-time monitored in the control center, as soon as a disturbance occurs, the amount of power lost by the tripped generators can be available. Therefore, the amount of power lost is compared to the amount of the available reserve capacity. If the amount of power lost is less than the amount of spinning reserve capacity, the load shedding plan is avoided; otherwise, the load shedding process cannot be avoided.

In general, the main principals of the proposed approach are summarized as follows:

- The frequency threshold of load shedding relays are adaptively adjusted. This task is performed in a wide-area manner.
- Fast changes in both the reactive power and voltage magnitude in all buses are effectively considered. Therefore, a new index is proposed to prioritize the shed loads.

At each step, the frequency settings are adaptively determined based on PMUs data. Considering the permissible frequency range, the frequency thresholds are represented by Eq. (16).

$$f_{setting} = \begin{cases} 49.7 & \left|\frac{df}{dt}\right|_{\max} \geq DF_2 \\ 49.4 + 0.025\left(\left|\frac{df}{dt}\right|_{\max} - DF_1\right) & DF_1 \leq \left|\frac{df}{dt}\right|_{\max} < DF_2 \end{cases} \tag{16}$$

Here, DF_1 is the maximum rate of frequency variations when the available reserve capacity accommodates the lost generation. Similarly, DF_2 represents the lower band of frequency setting in the case of large disturbances. As the frequency and its rate of change are incorporated in the proposed approach, a proper evaluation of the frequency/rotor-angle stability is performed, too. In some cases, the power system is faced with the frequency oscillations. As well, the outage of small generating units contributes to small decrease of power system frequency. However, in these sorts of disturbances, there is enough reserve capacity which effectively restores the power system, without any need to trigger the load shedding process. Thus, in such conditions, to prevent the load shedding initiation, a tolerable frequency threshold is considered.

The main idea deals with the voltage drop across the Thevenin equivalent generator impedance, behind a specific bus. How much the voltage drop gets higher, that bus is recognized as a potent one to stimulate the instability. The governing mathematical basis is represented by Eqs. (17)–(19).

$$\frac{P + jQ}{\overline{V}} = I^* = (p + jQ)Z^*_{Thev} = V(E - V)^* \tag{17}$$

$$VSI = \frac{\Delta V_k}{V_k} \tag{18}$$

$$\Delta V_k = |E_k - V_k| \tag{19}$$

Herein, E_k and Z_{Thev} are the Thevenin equivalent generator's voltage and impedance, respectively. Also, V_k is the voltage magnitude at bus k. Given Eq. (17), with the availability of the voltage and power consumption and calculation of Z_{Thev}, the value of the Thevenin equivalent voltage can be calculated to compute the voltage drop at each busbar. However, the proposed index may encounter with a technical obstacle in calculating the reactive power losses on the Thevenin equivalent generator's impedance. In order to avert this issue, the proposed index is rearranged based on Eq. (20).

$$\Delta VSI = \frac{E_k - V_{Li}}{V_{Li}} - \frac{E_k - V_{L0}}{V_{L0}} = \frac{E_k}{V_{L0}}\left(\frac{V_{L0} - V_{Li}}{V_{Li}}\right) \tag{20}$$

E_k and Q_{Thev} are equal with their pre-fault values. As mentioned earlier, the reactive power variation at each bus exhibits a faster response rather than its voltage magnitude.

Hence, a new index called as reactive power sensitivity, is developed by QSI. Similar to VSI, the QSI is calculated based on Eq. (21).

$$QSI = \frac{Q_{Thev} - Q_{Li}}{Q_{Li}} \tag{21}$$

How much the reactive power losses at the Thevenin equivalent generator's impedance are closer to the reactive power consumption in a specific bus, that point is recognized as a more potent one to incite the instability. Similar to ΔVSI, the ΔQSI is proposed based on Eq. (22).

$$\Delta QSI = \frac{Q_{Thev} - Q_{Li}}{Q_{Li}} - \frac{Q_{Thev} - Q_{L0}}{Q_{L0}} = \frac{Q_{Thev}}{Q_{L0}} \left(\frac{Q_{L0} - Q_{Li}}{Q_{Li}} \right) \tag{22}$$

This index is representing the variations of QSI prior and following the disturbances. As it is discussed, the greater reactive power losses are in line with buses more subjected to instability experience. Consequently, how much ΔQSI holds a greater value, that bus is more potent to stimulate the power system instability. This notice is easily observed in induction motors with their impressive effects in voltage stability.

Thus, the proposed approach can be extended as follows. How much the ratio of reactive power to the voltage magnitude variations gets higher, that bus is highly driven toward the instable regions. For the case of two distinct buses with similar voltage variations, the bus with higher reactive power variation is more subjected to instability. This idea is included in the proposed approach. Hence, in recovery of the same voltage drop, it requires more reactive power consumption from the network and given the disturbance occurrence and lack of sources power, the grid will be more likely to collapse. According to Eqs. (20) and (22) and with the approximate constant assumption of $\frac{E_k}{V_{L0}}$ and $\frac{Q_{Thev}}{Q_{L0}}$, the improved wide-area load shedding scheme is founded in the form of Eq. (23) (based on [25–35] and similar to the voltage-reactive power sensitivity in the Modal analysis).

$$QVSI = \frac{Q_{Li} - Q_0}{V_{Li} - V_0} \tag{23}$$

At each bus, if the frequency threshold is over-passed, Q_{Li} and V_{Li} are denoting the consumption reactive power and voltage magnitude at *i-th* bus. As well, Q_{L0} and V_{L0} correspond to the pre-contingency instant. A brief glossary on the preceding discussions reveals that following each disturbance, the buses with greater $QVSI$ index are highly concerned with instability occurrence. Encountering the outages in generating units, how much a bus is located far from the remaining generators, its short-circuit impedance increases. Thus, a higher reactive power variation is seen on that bus. This case is also reflected in the proposed index by assessing the reactive power variations. Moreover, the local characteristics of loads are in close relation with the voltage and reactive power variations in their coupling buses. As well, in the case of outages, on-load tap-changing transformers (OLTCs) are contributing to higher voltage drops and are adding to reactive power losses. In this case, a higher voltage drop with

a higher reactive power variation is recorded at the connecting buses. Furthermore, the activation of over-excitation limiter (OEL) curbs the remaining generating units from extra support of reactive power and thus, the instability deteriorates. As can be seen, the OLTC's and OEL's presence affects the power system with reactive power and voltage variations. The proposed index includes both of these variables and thus, represents a dependable index in load shedding process.

Moreover than the adaptive responses, the other eminent features of the proposed approach could be named as capturing a wide-area information regarding the overall system, low computational burden, and a fast response mechanism. A swift calculation of $QVSI$ results in a reliable and fast-response approach, preserving the power system stability. As established in Eq. (16), the proposed approach considers a frequency threshold (adaptively adjusted based on disturbances) and its rate of change to assess the load shedding initiation time. This timing point and the speed of process would be different for any specific power system and disturbance. Following this point and facing with generation shortages, the voltage and reactive power variations show a particular decremental trend, based on which the load shedding decisions are made. The flowchart of the proposed scheme is demonstrated in Fig. 2.

In contrast to the available mechanisms, the frequency thresholds of load shedding relays are adaptively adjusted. This task is performed in a wide-area manner. Fast changes in both the reactive power and voltage magnitude in all buses are effectively considered. The wide-area low computational burden of the proposed approach results in a fast-response shedding operation. Thus, an effective approach is achieved for stability enhancement.

4 Numerical analysis and discussions

In order to interrogate the performance of the proposed approach, a real test system is implemented in Power Factory-DigSILENT 14.1.3 platform. The implemented system, shown in Fig. 3, is a part of Iran transmission grid called as Khorasan network. This network embraces a total generation capacity of 2370 MW and contains 75 transmission buses. Different scenarios are devised to assess the performance of the proposed index, compared with the existing approaches. For the sake of clarity, the conventional method which is abbreviated by (M1), voltage magnitude by (M2), Modal analysis by (M3), and the proposed approach by (M4) are numerically analyzed. In conventional approach, only 100 ms is included as the operating time delay of each relay. However, for both of the Modal analysis and the proposed adaptive approach, 100 ms is considered as the relaying operation time and 100 ms is included as the communication delay toward the control center. Three different disturbances are explored in numerical simulations, based on which, a detailed analysis is conducted.

4.1 First disturbance: outage of all units in Neyshaboor power plant

In this event, the total generating capacity of Neyshaboor power plant, equal to 906 MW, is tripped at t = 0.1 s. Figure 4a, b are illustrating the voltage and frequency variations in some important buses. As can be seen, without any control action, the

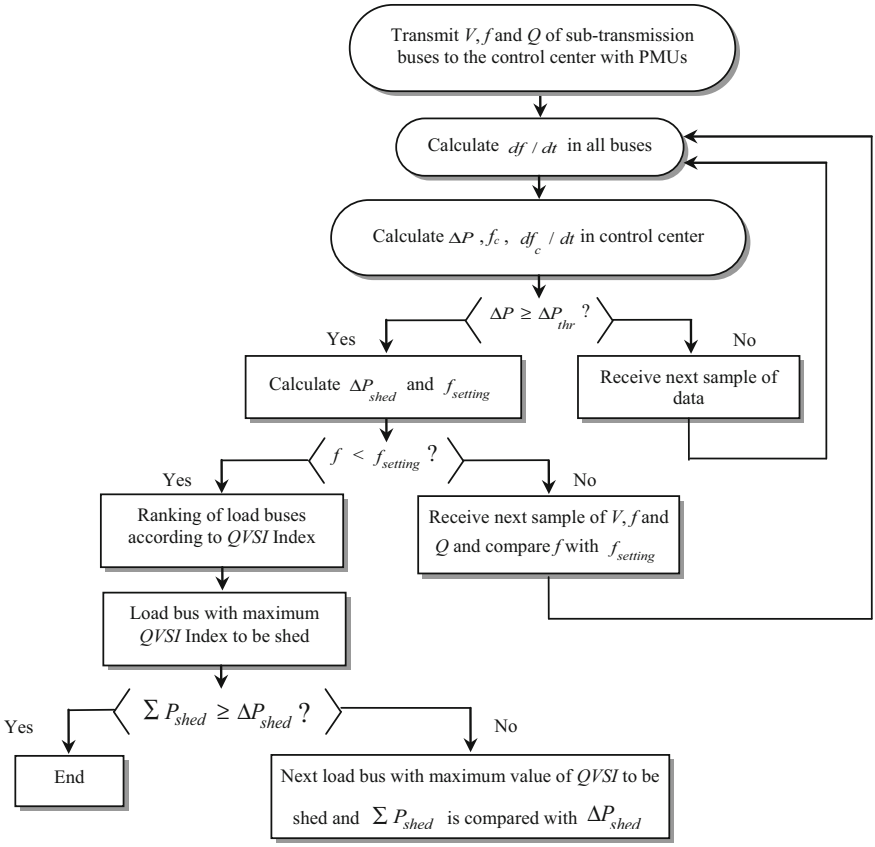

Fig. 2 Flowchart of the proposed load shedding approach based on $QVSI$ index

system is faced with both voltage and frequency instabilities. Thus, a reliable scheme is required to preserve the power system stability.

All of the investigated strategies, denoted by M1, M2, M3, and M4 are applied to the investigated test system to retrieve the voltage and frequency stabilities. By this way, the average values of voltage and frequency signals are displayed in Fig. 5a, b. For the sake of clarity, Fig. 5c, d are representing the enlarged illustrations around the load shedding instant. With respect to these figures, it is evidently observed that both of the voltage and frequency stabilities are retrieved, absolutely. However, the proposed index, denoted by M4, provides a more suitable response.

If a fine attention is paid on Fig. 5a–d, it can be seen that an improper selection of shed loads brings about weakly-damped transient and steady-state fluctuations in voltage and frequency signals. In other words, an erroneous load shedding pattern could instigate the power system fluctuations [36]. However, such oscillations, if to happen, could be suppressed by retuning the gains of governors and power system stabilizers. It should be mentioned that these oscillations could be a plausible origin of instability, themselves. This is while; a more uniform and stable response is observed

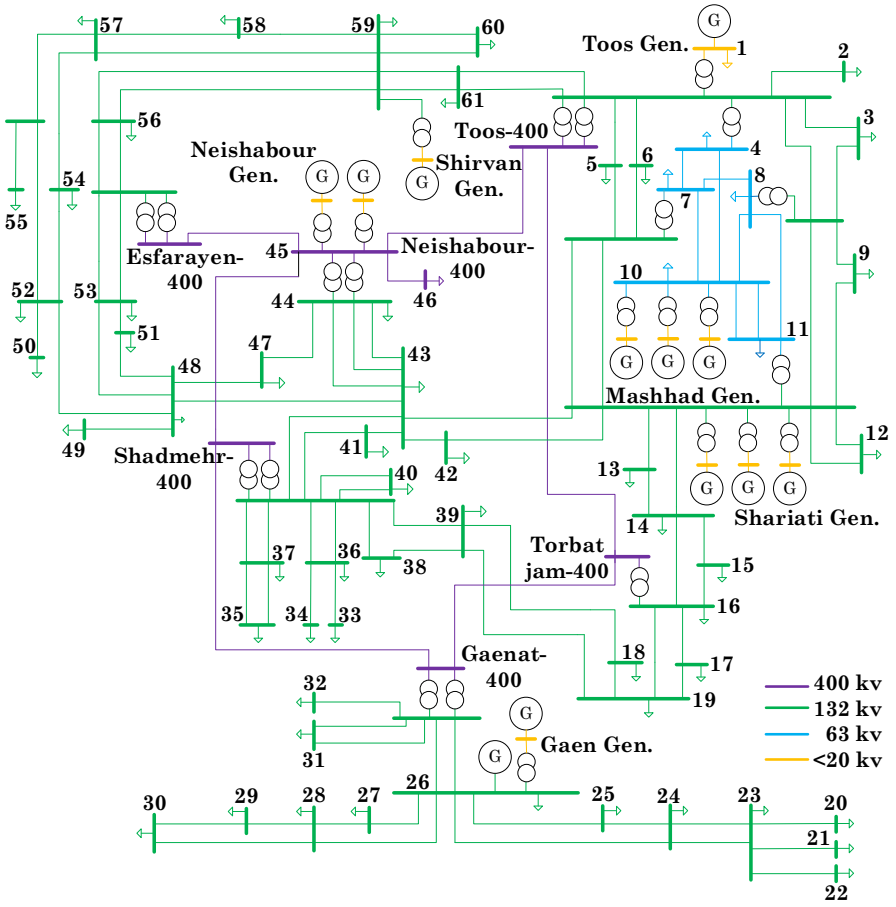

Fig. 3 Single-line diagram of the Khorasan transmission network

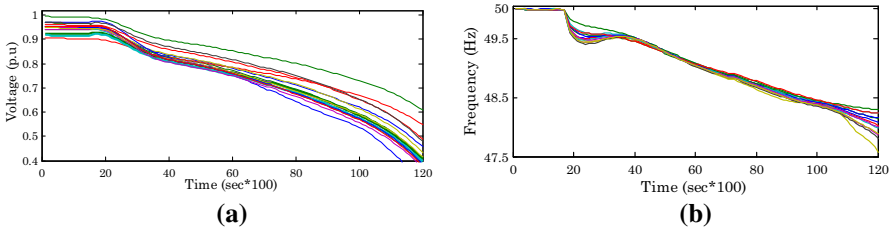

(a) **(b)**

Fig. 4 **a**, **b** Voltage and frequency variations at important buses following the first disturbance

by the proposed method. The proposed approach selects the bus numbers 7, 8, 11, 23, 26, 43, and 46 to perform the load shedding practice. Thus, suitable control signals are transferred to corresponding relays which include the amount of shed loads, too. Figure 6a–h are representing the frequency and propagated control signals. This process is applied on these buses at a specific time and via synchronized control signals. It is

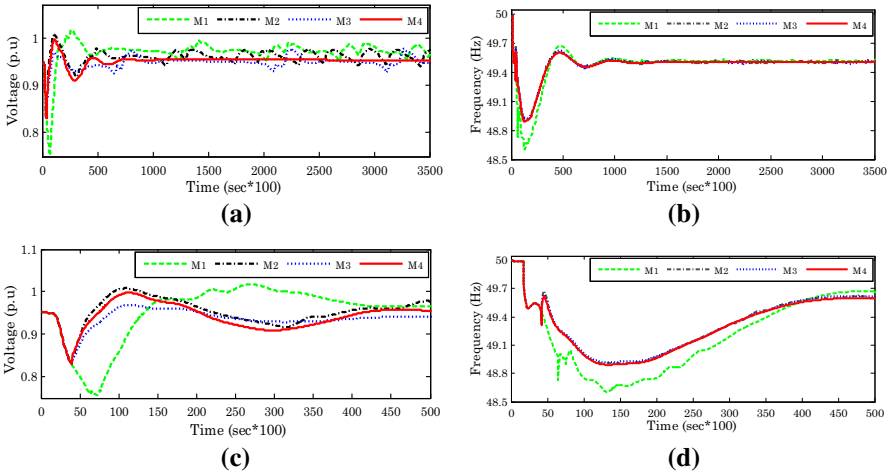

Fig. 5 **a**, **b** Average values of voltage and frequency signals for different load shedding schemes, **c**, **d** enlarged representations of the voltage and frequency signals, respectively

evidently recognized that by deploying the proposed approach, the frequency signal is retrieved to the stable conditions, successfully.

4.2 Second disturbance: combinatorial outage of Toos power plant and 400 kV Toos–Neyshaboor tie-line

In this event, the outage of Toos power plant instigates 560 MW generation shortage following which the 400 kV Toos–Neyshaboor tie-line is tripped, too. Next to this event, the voltage and frequency instabilities are recorded, which are shown in Fig. 7a, b.

In a similar approach, the implemented load shedding schemes are explored to assess the power system responses. The obtained results are shown in Fig. 8a–d. As can be seen, the Modal analysis and the conventional strategies could not afford the combinatorial events and thus, the voltage and frequency instabilities are reflected. Moreover, neglecting the variations in voltage and reactive power are also contributing to unstable responses. Contrarily, both the voltage magnitude and the proposed approaches are assuring stable responses, obtained for the voltage and frequency signals. Again, the superior performance of the proposed index is noticed over the voltage magnitude index. Not only the proposed approach demonstrates the best performance, but also it contributes to the least amount of shed load.

In this disturbance, the frequency signal is adaptively tuned based on the proposed approach. Based on this mechanism, the threshold frequency is tuned at 49.7 Hz, while in two step approach it is settled at 49.4 Hz. Figure 9a–d are granting the superior performance of the proposed approach over the two step frequency adjustments.

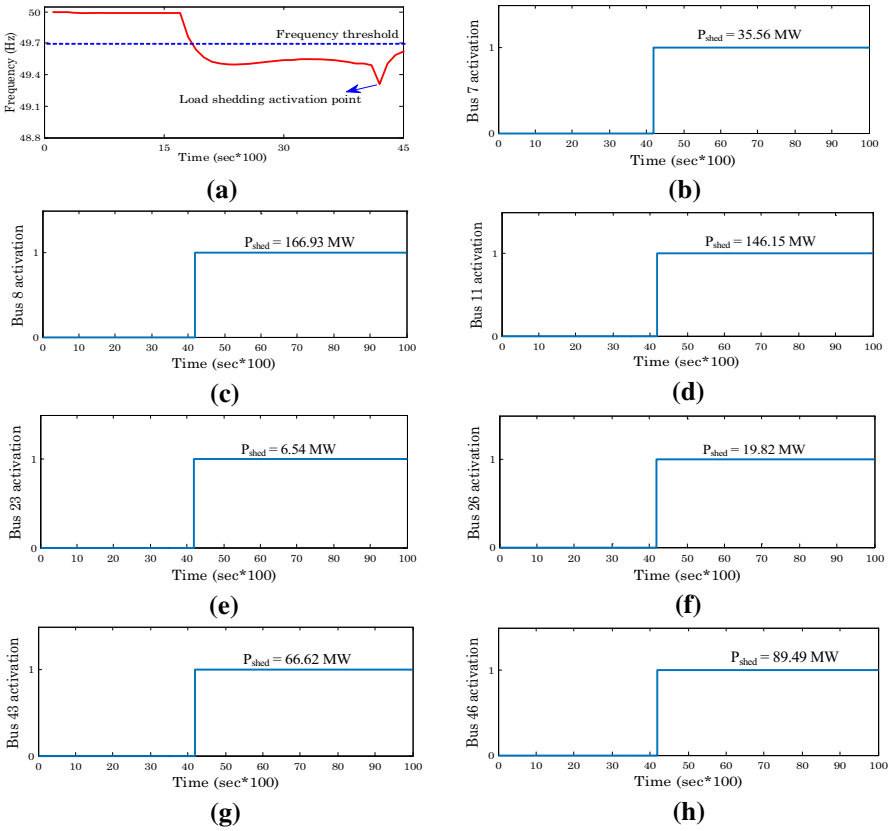

Fig. 6 **a** The average value of frequency signal, **b**–**h** the control signals transferred to buses 7, 8, 11, 23, 26, 43, and 46, respectively

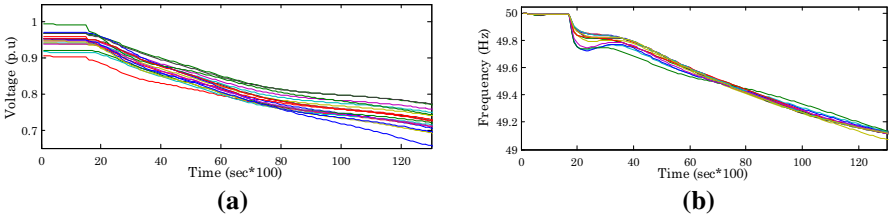

Fig. 7 **a**, **b** Voltage and frequency variations at important buses following the second disturbance

4.3 Third disturbance: a severe combinatorial outage of Toos power plant, two generation units of Sharyati power plant, and 400 kV Toos–Neyshaboor tie-line

In this event, the power system experiences the outage of Toos and Sharyati power plants, respectively with 560 and 212.12 MW capacities. Moreover, the 400 kV

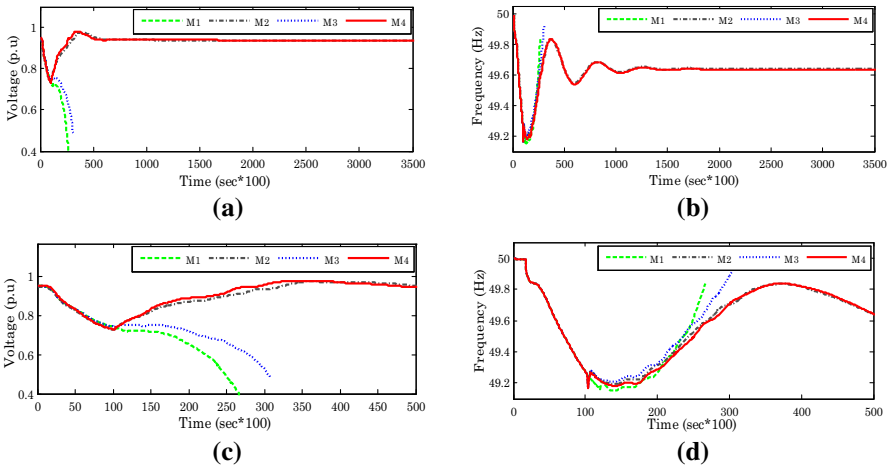

Fig. 8 **a**, **b** Average values of voltage and frequency signals for different load shedding schemes, **c**, **d** enlarged representations of the voltage and frequency signals, respectively

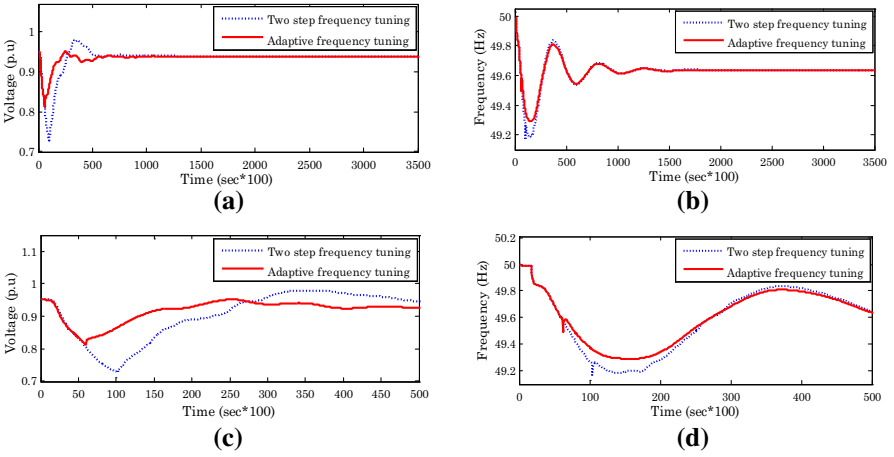

Fig. 9 **a**, **d** Average values of voltage and frequency signals recorded for adaptive and two-step frequency tuning approaches, **c**, **d** enlarged representations of the voltage and frequency signals, respectively

Toos–Neyshaboor tie-line is disconnected. Figure 10a, b are demonstrating the voltage and frequency collapse following this event.

As this event is recognized as a severe one, the frequency thresholds in both of the Modal and proposed approaches are set at 49.7 Hz. The obtained results are shown in Fig. 11a–d. As can be seen, in severe disturbances, the conventional load shedding method loses its validity to preserve the power system stability. Although 732.59 MW load is shed, however, the power system is not granted against the instability. In contradiction, wide-area adaptive approaches are preserving the voltage and frequency stabilities, effectively. Among these, the proposed index demonstrates a less amount of shed load with a superior and dependable performance.

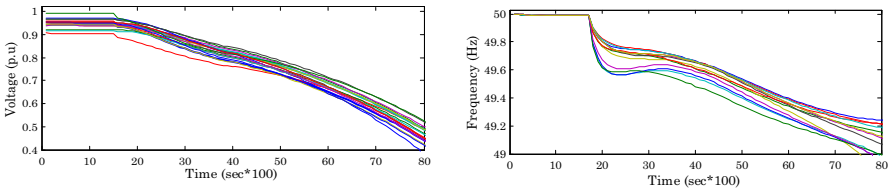

Fig. 10 **a**, **b** Voltage and frequency variations at important buses following the third disturbance

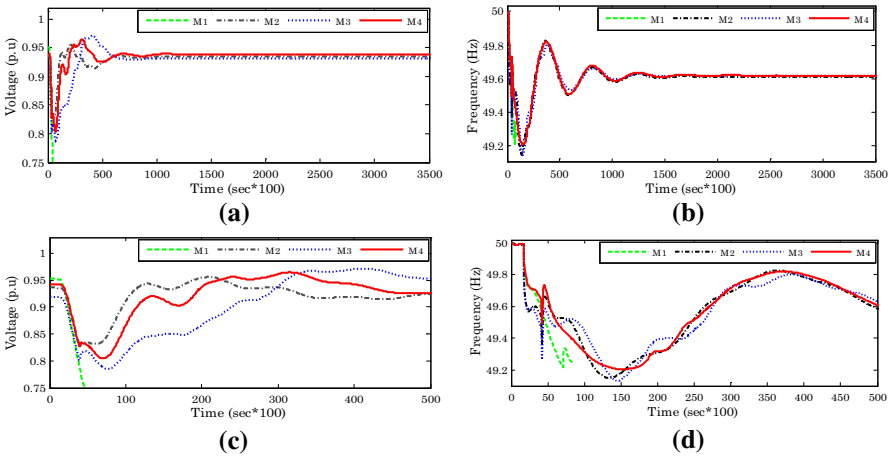

Fig. 11 **a**, **b** Average values of voltage and frequency signals for different load shedding schemes, **c**, **d** enlarged representations of the voltage and frequency signals, respectively

Considering the investigated disturbances, Table 1 summarizes the obtained results for the implemented load shedding schemes. For the investigated test system, the boundary value for m is determined as 1.4 Hz/s. Thus, the lower df/dt values represent the small disturbances, whereas the greater values denote the large disturbances. In the case of different power systems, the amount of m needs to be determined, exactly. In adaptive approaches, inclusion of the factor of 1.05 in Eq. 7 results in negligible increase of shed load. Disturbance 1 represents such a case. As clarified earlier, this modification averts the probable generation-consumption mismatches due to the unexpected reductions in reserve capacity. Another interesting observation is captured, contrarily. Considering disturbance 3, conventional method assigns 300 MW higher shed loads, compared to the adaptive approaches. Although a higher load is shed, the power system collapse is recorded. Thus, the conventional approach does not assure the power system stability, more obviously for combinatorial events. In contradiction, through a smaller amount of shed load, the adaptive approaches stabilize the power system. Such a notice approves the outperformance of adaptive approaches for different types of disturbances. In regards of the adaptive approaches, although the voltage magnitude-based approach retrieves the power system stability, the steady state oscillations are persistent in the system. As mentioned earlier, this point could

be an origin of instability, itself. In the case of Modal analysis, an acceptable response is obtained in preserving both the voltage and frequency stabilities. However, this approach is in-line with higher computational burden. This point inspires the power system instability in fast-propagated load variations. Moreover, the existing schemes could not accommodate the fast loading variations in load shedding solutions. To provide a swift control action, the voltage magnitude-based approach utilizes the pre-fault network data, which depreciates its overall functionality. This is while; the proposed approach considers the fast loading variations to improve the voltage and frequency stabilities. More interestingly, this notice is accompanied with smaller shed loads to grant the voltage and frequency margins. Furthermore, higher average values of voltage and frequency signals are attained which improves the power quality metrics. Also, the proposed approach moderates the computational burden of the process and founds a suitable option for real-time applications.

The performances of M1–M4 methods related to voltage and frequency stabilities are different. In many cases, the existing load shedding strategies could not afford the combinatorial events and thus, the voltage and frequency instabilities are reflected (disturbances 2 and 3). Therefore, it is necessary to use a method that considers the combination of voltage and frequency instabilities. Also, adapting and combining the under voltage and frequency load shedding relays are important issues that are considered in the proposed load shedding strategy. Better recovery of the voltage and frequency signals with the least amount of shed load is a significant result that can be achieved in the proposed method. To confirm the consistency of the simulation results with the mathematical basis of the proposed approach, further analysis is included as well. Figure 12 demonstrates the recorded values of QVSIs obtained for the investigated disturbances. As can be seen, sub-figure (a) corresponds to disturbance 1 in Table 1. It can be easily recognized that the selected buses in load shedding process contain greater QVSI values. Such a notice is captured for buses 7, 8, 11, 23, 26, 43, and 46. Based on sub-figures (b) and (c), a similar conclusion is made in regards of buses 8 and 11 and also 8, 11, 35, and 46, respectively for the second and third disturbances. Thus, the validity of the proposed approach is deduced.

5 Concluding remarks

This study established a new wide-area adaptive load shedding scheme for effective retrieving of power system voltage and frequency stabilities. The proposed approach deployed the wide-area data provided by PMUs. As a faster indicator of power system stability, reactive power variation was included in the proposed $QVSI$ index. As well, the fast loading variations, recorded in pre- and post-disturbance points, have also been included. This issue enhanced the functionality of the proposed approach in stability analysis. In this practice, the frequency settings of relays have been adaptively adjusted based on the magnitude of each disturbance. Hence, rather than a constant response, a suitable load shedding pattern was achieved based on the severity of the events. The proposed approach was shown to be effective in sever and combinatorial disturbances, where the conventional methods failed to provide a stable response. In the case of voltage magnitude-based approach, although a stable response was

Table 1 Comparison of the investigated mechanisms for load shedding procedure

Event	Comparison point							
	Severity	Load shedding scheme	Minimum frequency (Hz)	Average frequency (Hz)	Minimum voltage(p.u)	Average voltage (p.u)	ΔP_{shedd} (MW)	Selected buses
Disturbance 1	8.84 (large)	Conventional	49.560	49.560	0.9481	0.9752	521.5	4-11-14-15-28-36-37-40-43-47-52-53-54-55
		Voltage magnitude	49.507	49.507	0.9003	0.9596	532.78	8-20-21-22-23-34-35-37-38-47-48-49-50-53-54
		Modal analysis	49.505	49.505	0.9037	0.9485	531.31	1-2-3-6-9-12-15-17-18-20-21-22-23-25-27-32-34-42-44-50-51-53-54-55-58-59-60
		Proposed	49.502	49.502	0.9040	0.9528	531.11	7-8-11-23-26-43-46
Disturbance 2	0.69 (small)	Conventional	Collapse	Collapse	Collapse	Collapse	158.7	15-40-47-53-54
		Voltage magnitude	49.639	49.639	0.9030	0.9334	208.7	2-8-20-21-22
		Modal analysis	Collapse	Collapse	Collapse	Collapse	210.45	3-35-46
		Proposed	49.637	49.637	0.9028	0.9494	207.35	8-11
Disturbance 3	4.44 (large)	Conventional	Collapse	Collapse	Collapse	Collapse	732.59	4-11-14-15-19-28-36-37-40-43-47-52-53-54-55-59-61
		Voltage magnitude	49.611	49.611	0.9088	0.9340	453.41	2-7-8-11
		Modal analysis	49.619	49.619	0.8849	0.9306	457.18	2-3-6-9-12-20-21-22-23-25-38-48-50-55-59-60
		Proposed	49.619	49.619	0.9035	0.9381	453.33	8-11-35-46

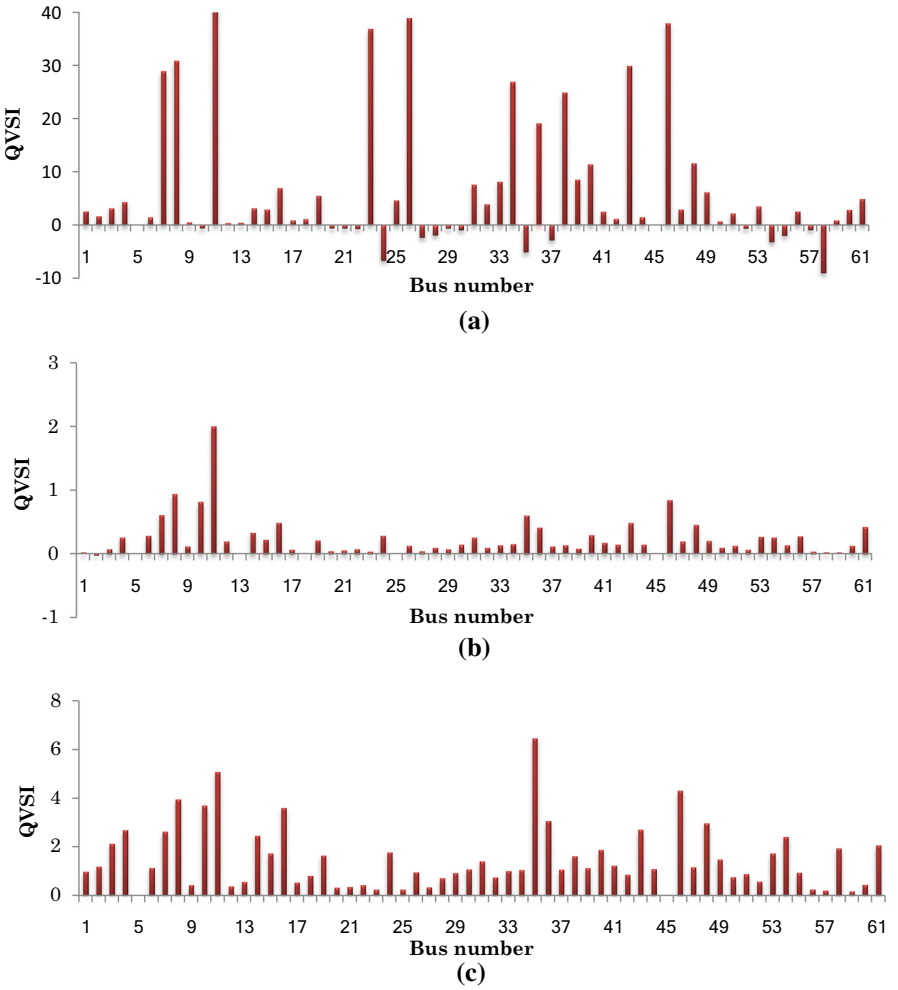

Fig. 12 **a–c** QVSI values in first, second, and third disturbances

noticed, however, the persistent oscillations could jeopardize the power system stability. Moreover, although the Modal analysis demonstrates acceptable response, it is characterized with high computational burden. This trend was shown to end in a similar load shedding scheme for different kinds of disturbances. Thus, in some cases, the unsuitable load shedding regime might trigger the voltage and frequency instabilities. In contradiction, the low computational effort by the proposed approach guaranteed a fast response on-line approach, which certified an effective and adaptive load shedding strategy.

The conducted study does not include the gradual load growth which overpasses the generation capacity. In this situation, a precise evaluation of the stability limit is necessary to determine the maximum loading capacity of the network. Moreover,

the proposed approach should be improved to consider the loads' dynamics in load shedding process. These issues are regarded as open research topics to be explored in more depth.

References

1. Kearsley, R.: Restoration in Sweden and experience gained from the blackout of 1983. IEEE Trans. Power Syst. **2**, 422–428 (1987)
2. U.S.-Canada Power System Outage Task Force: Final report on the August 14, 2003 blackout in the United States and Canada: causes and recommendations (2004)
3. Kundur, P., Paserba, J., Ajjarapu, V., Andersson, G., et al.: IEEE/CIGRE joint task force on stability terms and definitions. Definition and classification of power system stability. IEEE Trans. Power Syst. **19**, 1378–1401 (2004)
4. Shekari, T., Aminifar, F., Sanaye-Pasand, M.: An analytical adaptive load shedding scheme against severe combinational disturbances. IEEE Trans. Power Syst. **31**, 4135–4143 (2016)
5. Horowitz, S.H., Phadke, A.G.: Boosting immunity to blackouts. IEEE Power Energy Mag. **99**, 47–53 (2003)
6. Mehrabi, K., Afsharnia, S., Golshannavaz, S.: Toward a wide-area load shedding scheme: adaptive determination of frequency threshold and shed load values. Int Trans. Electr. Energ. Syst. **28**, e2470 (2018)
7. Eremia, M., Shahidehpour, M.: Handbook of Electrical Power System Dynamic: Modeling, Stability and Control. Wiley-IEEE, Oxford (2013)
8. Taylor, C.W.: Concepts of undervoltage load shedding for voltage stability. IEEE Trans Power Del **7**, 480–488 (1992)
9. Jonsson, M.: Protection Strategies to Mitigate Major Power Systems Breakdowns. Chalmers University of Technology, Göteborg (2003)
10. Dai, Y., Xu, Y., Dong, Z.Y., Wong, K.P., Zhuang, L.: Real-time prediction of event-driven load shedding for frequency stability enhancement of power systems. IET Gen. Transm. Distrib. **6**, 914–921 (2012)
11. Goubko, M., Ginz, V.: Improved spectral clustering for multi-objective controlled islanding of power grid. Energy Syst. **4**, 1–36 (2017)
12. Fan, N., et al.: A mixed integer programming approach for optimal power grid intentional islanding. Energy Syst. **3**, 77–93 (2012)
13. Golari, M., Fan, N., Wang, J.: Large-scale stochastic power grid islanding operations by line switching and controlled load shedding. Energy Syst. **8**, 601–621 (2017)
14. Council, Western Electricity Coordination: Undervoltage Load Shedding Guidelines. Undervoltage Load Shedding Task Force (UVLSTF), Technical Studies Subcommittee, Salt Lake City (1999)
15. Begovic, M., Fulton, D., Gonzalez, M.R., Goossens, J.: Summary of system protection and voltage stability. IEEE Trans. Power Del. **10**, 631–638 (1995)
16. Terzija, V.V., Koglin, H.J.: New approach of adaptive automatic load shedding. Eur. Trans. Electr. Power **11**, 329–334 (2001)
17. Delfino, B., Massucco, S., Morini, A., Scalera, P., Silvestro, F.: Implementation and comparison of different underfrequency load shedding schemes. In: Proc. 2001 IEEE Power Engineering Society Summer Meeting, Vancouver, Canada, pp. 307–312 (2001)
18. Parniani, M., Nasri, A.: SCADA based under frequency load shedding integrated with rate of frequency decline. In: Proc of IEEE Power Engineering Society General Meeting, Montreal, Que., Canada (2006)
19. Ahsan, M.Q., Chowdhury, A.H., Ahmed, S.S., Bhuyan, I.H., Haque, M.A., Rahman, H.: Technique to develop auto load shedding and islanding scheme to prevent power system blackout. IEEE Trans. Power Syst. **27**, 198–205 (2013)
20. Abdelwahid, S., Babiker, A., Eltom, A., Kobet, G.: Hardware implementation of an automatic adaptive centralized underfrequency load shedding scheme. IEEE Trans. Power Del. **29**, 2664–2673 (2014)
21. Hoseinzadeh, B., Da Silva, F.M.F., Bak, C.L.: Adaptive tuning of frequency thresholds using voltage drop data in decentralized load shedding. IEEE Trans. Power Syst. **30**, 2055–2062 (2015)

22. Rudez, U., Mihalic, R.: Predictive underfrequency load shedding scheme for islanded power systems with renewable generation. Electr. Power Syst. Res. **126**, 21–28 (2015)
23. Girgis, A.A., Mathure, S.: Application of active power sensitivity to frequency and voltage variations on load shedding. Electr. Power Syst. Res. **80**, 306–310 (2010)
24. Hooshmand, R., Moazzami, M.: Optimal design of adaptive under frequency load shedding using artificial neural networks in isolated power system. Int. J. Electr. Power Energy Syst. **42**, 220–228 (2012)
25. Gong, Y., Schulz, N., Guzman, A.: Synchrophasor-based real-time voltage stability index. In: Proc. 2006 Power System Conference & Exposition, Atlanta, GA, USA, pp. 1029–1036 (2006)
26. Seethalekshmi, K., Singh, S.N., Srivastava, S.C.: A synchrophasor assisted frequency and voltage stability based load shedding scheme for self-healing of power system. IEEE Trans. Smart Grid **2**, 221–230 (2011)
27. Milosevic, B., Begovic, M.: Voltage-stability protection and control using a wide-area network of phasor measurements. IEEE Trans. Power Syst. **18**, 121–127 (2003)
28. Corsi, S., Taranto, G.N.: A real-time voltage instability identification algorithm based on local phasor measurements. IEEE Trans. Power Syst. **23**, 1271–1279 (2008)
29. Gao, B., Morison, G.K., Kundur, P.: Voltage stability evaluation using modal analysis. IEEE Trans. Power Syst. **4**, 1529–1542 (1992)
30. Morison, G.K., Gao, B., Kundur, P.: Voltage stability analysis using static and dynamic approaches. IEEE Trans. Power Syst. **8**, 1159–1171 (1993)
31. Jones, J.R., Kirkland, W.D.: Computer algorithm for selection of frequency relays for load shedding. IEEE Comput. Appl. Power **1**, 21–25 (1988)
32. Seyedi, H., Sanaye-Pasand, M.: New centralized adaptive load-shedding algorithms to mitigate power system blackouts. IET Gen. Transm. Distrib. **3**, 99–114 (2009)
33. Kundur, P.: Power System Stability and Control. McGraw-Hill, New York (1994)
34. Tang, J., Junqi, L., Ferdinanda, P., Antonello, M.: Adaptive load shedding based on combined frequency and voltage stability assessment using synchrophasor measurements. IEEE Trans. Power Syst. **28**, 2035–2047 (2013)
35. Corsi, S.: Wide area voltage protection. IET Gen. Transm. Distrib. **4**, 1164–1179 (2010)
36. Wu, C., Gao, L., Dai, Y.: Simulation and optimization of load shedding scheme for islanded power system. In: International Conference on Power System Technology (POWERCON), Hangzhou, pp. 1–6 (2010)